Gallium Maltolate Inhibits Human Cutaneous T-Cell Lymphoma Tumor Development in Mice

Xuesong Wu[1], Timothy W. Wang[1], George M. Lessmann[2], Jamal Saleh[1], Xiping Liu[1], Christopher R. Chitambar[2] and Sam T. Hwang[1]

Cutaneous T-cell lymphomas (CTCLs) represent a heterogeneous group of non-Hodgkin's lymphoma characterized by an accumulation of malignant CD4 T cells in the skin. The group IIIa metal salt, gallium nitrate, is known to have antineoplastic activity against B-cell lymphoma in humans, but its activity in CTCLs has not been elaborated in detail. Herein, we examined the antineoplastic efficacy of a gallium compound, gallium maltolate (GaM), *in vitro* and *in vivo* with murine models of CTCLs. GaM inhibited cell growth and induced apoptosis of cultured CTCL cells. In human CTCL xenograft models, peritumoral injection of GaM limited the growth of CTCL cells, shown by fewer tumor formations, smaller tumor sizes, and decreased neovascularization in tumor microenvironment. To identify key signaling pathways that have a role in GaM-mediated reduction of tumor growth, we analyzed inflammatory cytokines, as well as signal transduction pathways in CTCL cells treated by GaM. IFN-γ-induced chemokines and IL-13 were found to be notably increased in GaM-treated CTCL cells. However, immunosuppressive cytokines, such as IL-10, were decreased with GaM treatment. Interestingly, both oxidative stress and p53 pathways were involved in GaM-induced cytotoxicity. These results warrant further investigation of GaM as a therapeutic agent for CTCLs.

Journal of Investigative Dermatology (2015) **135,** 877–884; doi:10.1038/jid.2014.476; published online 11 December 2014

INTRODUCTION

Cutaneous T-cell lymphomas (CTCLs) are a heterogeneous group of peripheral, extranodal, non-Hodgkin's lymphomas, resulting in a variety of skin findings, including scaly red patches, plaques, tumors, and erythroderma (Hwang *et al.*, 2008). Patients with tumor stage disease have a poor prognosis with a 5-year survival of less than 50%. The treatment of CTCLs ranges from skin-directed therapies for early disease to more complex chemotherapy-based treatments for later stages (Hwang *et al.*, 2008). Cures are not usually seen, however, and patients require on-going therapy. Hence, there is a great need to continue to develop effective drugs for the treatment of CTCLs.

Mounting evidence indicates that an inflammatory environment is a participatory component of tumor development (Mantovani *et al.*, 2008). In one of our established murine models of CTCLs, C57BL/6 mice injected with MBL2 T-lymphoma cells in the ear can be induced to develop a cutaneous lymphoma in the setting of an inflammatory response generated by a single topical application of 2,4-Dinitro-fluorobenzene (Wu *et al.*, 2011). In this model, tumors do not develop in these animals in the absence of 2,4-Dinitro-fluorobenzene application or when mice are treated with corticosteroids, thus underscoring the importance of the inflammatory microenvironment in this model of CTCL. Moreover, inflammatory macrophages appear to have a critical role, as depletion of macrophages markedly reduces the size of the T-cell tumors (Wu *et al.*, 2014)

Gallium is a group IIIa metal that shares certain chemical similarities with iron (III). These properties enable gallium to bind to the iron transport protein transferrin and to be taken up by cells via transferrin receptor (TfR)-mediated endocytosis of transferrin-gallium (Tf-Ga) complexes (Larson *et al.*, 1980, Harris and Pecoraro, 1983, Chitambar and Zivkovic, 1987). Lymphoma cells are known to express high densities of cell surface TfRs, thus making them selective targets for Tf-Ga (Kvaloy *et al.*, 1984, Chitambar *et al.*, 1989). In contrast to lymphoma cells, normal resting lymphocytes do not express cell surface TfRs and are thus not targeted by Tf-Ga (Chitambar *et al.*, 1989). Tf-Ga interferes with the cellular uptake of transferrin-iron, producing a state of cellular iron deprivation, which can induce apoptosis (Chitambar *et al.*, 1989). Malignant cells have a greater requirement for iron compared with normal cells, rendering them more susceptible to iron deprivation (Richardson *et al.*, 2009). The action of gallium extends beyond interfering with TfR-mediated iron uptake; it inhibits iron-dependent ribonucleotide reductase (deoxyribonucleotide

[1]*Department of Dermatology, Medical College of Wisconsin, Milwaukee, Wisconsin and* [2]*Department of Medicine, Division of Hematology and Oncology, Medical College of Wisconsin, Milwaukee, Wisconsin*

Correspondence: Sam T. Hwang, Department of Dermatology, Medical College of Wisconsin, 9200 West Wisconsin Avenue, Milwaukee, Wisconsin 53226, USA. E-mail: sthwang@mcw.edu

Abbreviations: CTCL, cutaneous T-cell lymphoma; GaM, gallium maltolate; GaN, gallium nitrate; PBS, phosphate-buffered saline; Tf-Ga, transferrin-gallium; TfR, transferrin receptor

Received 17 March 2014; revised 22 September 2014; accepted 20 October 2014; accepted article preview online 5 November 2014; published online 11 December 2014

synthesis), iron-dependent mitochondrial function, and other processes in the cells, ultimately culminating in cell death (Chitambar, 2012; Chitambar and Antholine, 2013). Gallium also has significant anti-inflammatory and immunosuppressive activities (Chitambar, 2010). The anti-inflammatory action of gallium appears to involve the downregulation of inflammatory T cells and macrophages, as well as possible interference with matrix metalloproteinases. Because many iron compounds are proinflammatory, the ability of gallium to act as a nonfunctional iron mimetic may contribute to its anti-inflammatory activity.

Clinical trials have shown gallium nitrate (GaN), a first generation gallium compound, to have significant antineoplastic activity in B-cell non-Hodgkin's lymphoma (Straus, 2003). However, drug resistance to GaN may be encountered, thus limiting its anti-tumor efficacy in some patients. Our recent studies have shown that gallium maltolate (GaM), a next generation of gallium compound, displays greater cytotoxicity compared with GaN against a panel of lymphoma cell lines, including lymphoma cells resistant to growth inhibition by GaN (Chitambar *et al.*, 2007). In contrast to GaN, which is a simple metal salt, GaM consists of three maltolate ligands bidentately bound to a central gallium atom in a propeller-like arrangement (Chitambar *et al.*, 2007). Gallium's anti-inflammatory properties may be relevant to CTCLs, as our studies have shown that CTCL develops in a background of inflammatory changes in the skin. Beyond a single case report of a marked response to GaN in a patient with peripheral T-cell lymphoma refractory to conventional therapy (Huang *et al.*, 2005), there are limited data and research on the efficacy of gallium compounds in CTCLs. In the present study, we examined the antineoplastic efficacy of GaM *in vitro* and *in vivo* in preclinical murine models of CTCLs and investigated the molecular mechanisms that mediate the anti-tumor activity of this metallocompound.

RESULTS

Cytotoxic activity of GaM in CTCL cells

Hut78 and HH are both CTCL cell lines that were established from human CTCL patients. Because TfR-mediated endocytosis of Tf-Ga is the initial step in gallium-mediated cell death, we first examined whether TfR was present on the surface of Hut78 and HH cells. Using anti-CD71 (TfR) antibody, we detected the homogeneous expression of TfR on both cell lines by flow cytometry (Supplementary Figure S1 online), indicating that these cells may be selectively targeted by TfR-Ga through TfR-ligand engagement. Next, we exposed both cultured cell lines to GaM at increasing concentrations (Figure 1a). Both CTCL cell lines exhibited dose-dependent cytotoxicity with GaM. Of note, a slight proliferative effect of GaM was seen after day 1 of treatment at 100 μM, but complete killing of Hut78 cells was seen after 3 days of incubation. The ability of gallium to mimic iron, an essential element for cell growth, may account for the initial proliferative effects of low-dose GaM. Although HH cells were also sensitive to GaM exposure, they required a higher concentration of GaM and a longer incubation period for complete killing (Figure 1a). In the flow cytometry–based apoptosis assay, Hut78 cells showed marked increases of annexin V or 7-AAD positivity after 1 day exposure to GaM at 100 μM (47.5% in GaM vs. 10.9% in phosphate-buffered saline (PBS control; Figure 1b). Interestingly, we noticed that GaM displayed only slight toxicity against HaCat keratinocyte cells (Supplementary Figure S2 online), suggesting that GaM may have selective toxicity toward the two malignant T-cell lines.

A Seahorse XF24 Extracellular Flux Analyzer (Seahorse Bioscience, North Billerica, MA) was utilized to measure oxygen consumption in CTCL cell lines. Incubation of HuT78 cells with increasing concentrations of GaM over 8 hours resulted in a dose-dependent decrease in the cellular oxygen consumption rate before measurable changes in cell death could be detected (Figure 1c), suggesting that an early event in gallium-induced tumor cell death involves inhibition of mitochondrial respiratory function, and thus cellular metabolism.

Inhibition of tumor growth by GaM in CTCL mouse models

In order to determine whether GaM can block tumor growth *in vivo*, we established xenograft CTCL mouse models through the subcutaneous (SC) implantation of CTCL cells, either Hut78 or HH cells, in the flank skin of Nod-Scid IL-2 γ-chain knockout (NSG) mice. Tumors were apparent after 2 weeks with most growth occurring during the third and fourth weeks. To observe the treatment effect by GaM, we injected GaM at the same site with a daily dosage of 400 μg per mouse for 5 days 1 day after tumor cell inoculation. Four weeks after implantation, mice were killed and examined (Figure 2a). Solid tumors were found in SC area in the mice in PBS-treated group, whereas tumors were rarely found in GaM-treated mice (Figure 2b). Significant decreases in tumor formation were revealed in both Hut78 and HH cell line experiments (Supplementary Figure S3 online, Hut78, $P=0.0021$, HH, $P=0.0061$).

In addition, we sought to determine the anti-tumor effect of GaM on established CTCL tumors. Therefore, instead of on day 2, we started GaM treatment on day 8 or 15 after tumor implantation as indicated (Figure 2a). Mice were killed 4 weeks after implantation. With treatment starting at day 8, tumor growth was greatly inhibited as confirmed by hematoxylin and eosin staining (Figure 2c). Even with treatment starting at day 15, the GaM-treated tumors showed a significant reduction in size compared with PBS treatment ($P=0.0415$), although tumor growth was only partially inhibited (Figure 2d and e). Thus, even in established tumors, GaM treatment can effectively inhibit growth of CTCL tumors in NSG mice (Figure 2d and e).

Decreased tumor vascularization with GaM treatment in tumor-bearing mice

To understand the impact of GaM treatment on the tumor environment, we first assessed tumor vascularity in Hut78 tumor tissues isolated from PBS or GaM-treated tumor-bearing mice. Immunofluorescent staining showed a significant decrease in CD31, a recognized marker for vascular endothelial cells, in the tumors from GaM-treated mice (Supplementary Figure S4a and b online). Although positive signals highlighting both small vessels and individual cells were frequently observed amidst condensed tumor area in the PBS control

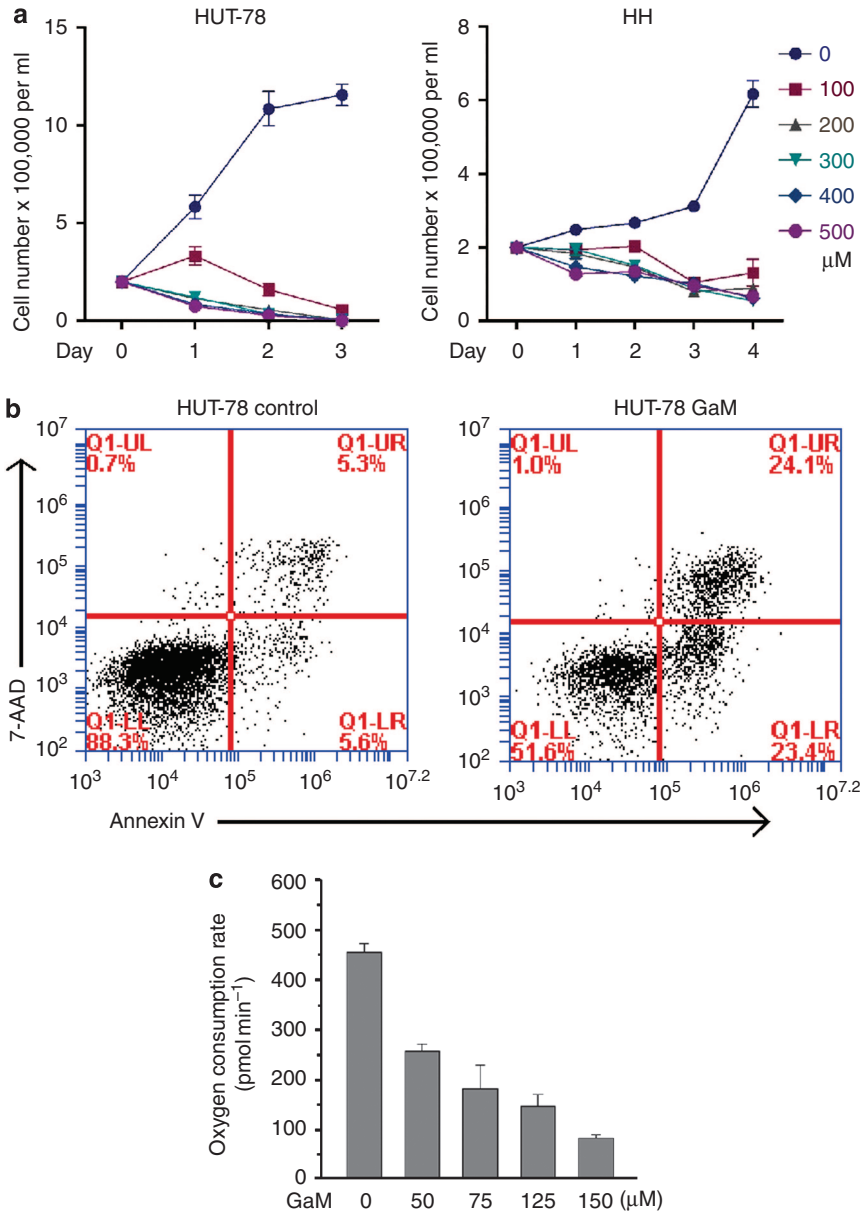

Figure 1. GaM has cytotoxic effects on cultured CTCL cells. (**a**) The trypan blue exclusion assay measuring the effect of GAM exposure on the growth rate of Hut78 and HH cells. Cells were incubated with GaM at indicated concentrations, and live cells were counted after trypan blue staining on day 0, 1, 2, and 3. (**b**) The apoptosis assay for GaM-treated Hut78 cells. Cultured Hut78 cells were exposed to GaM at 100 μM for 1 day. Cells were stained with Annexin V and 7-AAD and analyzed by FACS. (**c**) GaM produces a dose-dependent decrease in the cellular oxygen consumption rate in HuT78 cells. Cells were incubated with GaM for 8 hours prior to assay. CTCL, cutaneous T-cell lymphoma; GaM, gallium maltolate.

group, we rarely identified equivalent signals in GaM-treated tumors, suggesting that angiogenesis was reduced in GaM-treated mice. Staining with antibodies against podoplanin, the lymphatic marker, or F4/80 (a macrophage marker) did not reveal differences between GaM-treated and control groups (Supplementary Figure S4 online). Thus, GaM treatment results in marked decreases in CD31 staining, suggesting that GaM interferes with tumor angiogenesis but not lymphangiogenesis (which may have a role in tumor spread to lymph nodes) or numbers of macrophages (which in prior studies were shown to potentially influence CTCL development (Sugaya *et al.*, 2012; Wu *et al.*, 2014).

GaM exposure induces production of cytotoxic inflammatory cytokines in Hut78 cells

In order to determine whether administration of GaM had broad systemic effects on host immunity, we analyzed major immune cell populations (macrophages and neutrophils) in spleens from mice after GaM treatment. Spleens were collected from the mice in the aforementioned treatment groups.

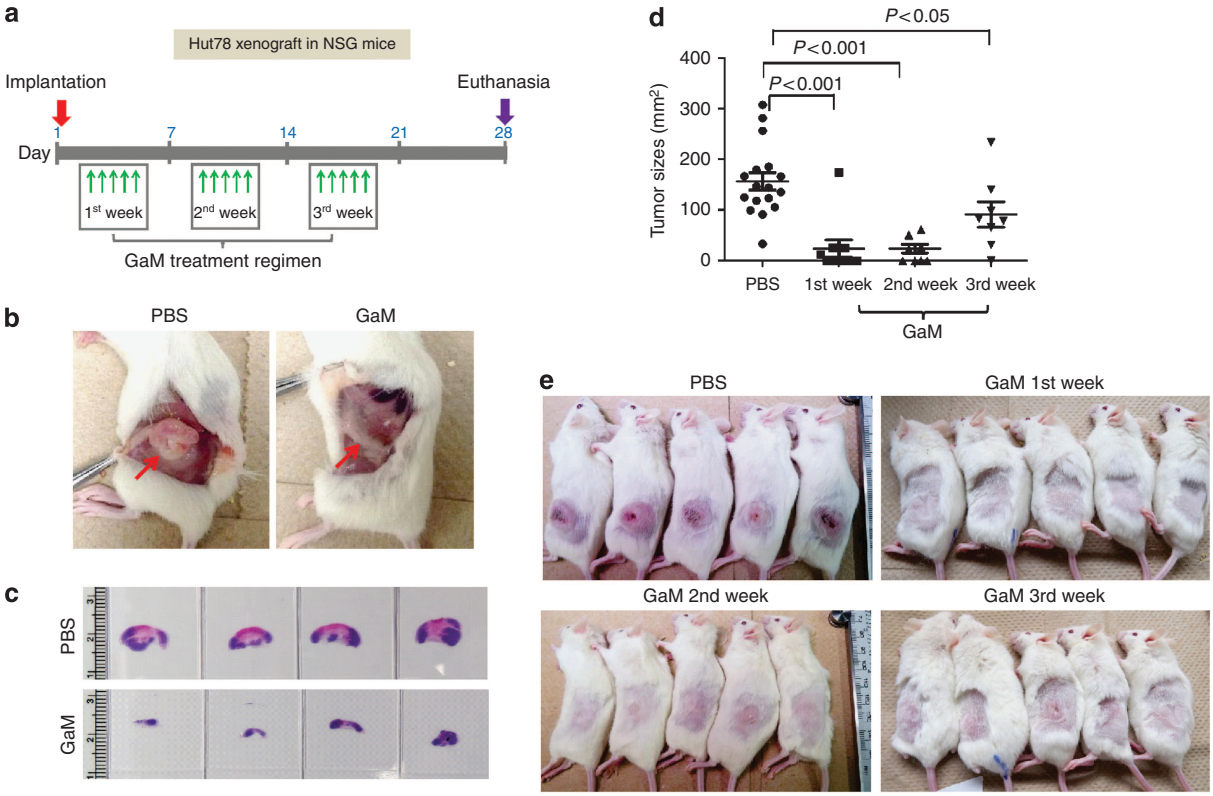

Figure 2. Administration of GaM inhibits CTCL tumor growth in mouse models. (**a**) Schematic GaM treatment regimen. Hut78 cells were implanted SC in NSG mice on day 1. GaM was administered by peritumoral injection at a dosage of 400 µg per mouse/day for 5 consecutive days starting on day 2 (1st wk), day 8 (2nd wk), or day 15 (3rd wk), respectively. Equal volume of PBS (200 µl) was injected instead of GaM for 1st wk as control. (**b**) Representative pictures of 1st wk GaM- and PBS-treated mice. Red arrows indicate subcutaneous areas where tumor formation was seen in PBS-treated, whereas not in GaM-treated mice. (**c**) H&E staining for maximum cross-sections of tumors isolated from GaM-treated (2nd wk) and control groups. (**d**) Sizes and (**e**) images of flank tumors 4 weeks after implantation. Student's *t*-test was performed between each GaM-treated group and PBS control. CTCL, cutaneous T-cell lymphoma; GaM, gallium maltolate; H&E, hematoxylin and eosin.

fluorescence-activated cell sorting (FACS) analysis revealed an equal percentage of $CD45^+$ cells in GaM and control groups. Further analysis for the two major immune populations, $F4/80^+$ macrophages and $Gr\text{-}1^+$ neutrophils, also did not reveal any differences among the treatment groups (Supplementary Figure S5 online).

Although broad systemic changes in host immunity were not observed, local changes in host immunity via regulatory cytokines might explain GaM anti-tumor activity. Therefore, to detect GaM-induced changes after GaM treatment, we performed pathway-focused microarray analysis of inflammatory cytokines on RNA extracted from Hut78 cells 1 day after treatment with either GaM or PBS. Interestingly, we detected upregulation of proinflammatory cytokines and receptors, such as CEBPB, CX3CR1, CXCL11, IL17C, IL1A, IL36A, TNF, XCR1, and, remarkably, IL-13. On the contrary, downregulation of IL-10 was detected in GaM-treated Hut78 cells, when compared with PBS control samples (Figure 3 and Supplementary Table S1 online). Of note, the Th1 IFN-γ-induced chemokines, CXCL10 (IP-10) and CXCL11, were both significantly upregulated with GaM treatment. It has been demonstrated that CXCL10 and CXCL11 are potent angiostatic proteins, whereas IL-10 promotes angiogenesis. Thus, the reduced vascularity observed in GaM-treated tumors may be mediated by regulation of chemokines and cytokines that regulate angiogenesis.

GaM-induced apoptosis involves the oxidative stress and p53 pathways

Given that direct cytotoxicity observed in tumor cells following GaM exposure, we further explored the involvement of signal transduction pathways in CTCLs following GaM treatment. We utilized mRNA expression microarrays that target genes for 10 common pathways important for developmental, immunological, metabolic, and stress-activated processes. The transcriptional profiles of Hut78 cells treated with GaM and PBS were compared in order to analyze differential activation of signaling pathways (Supplementary Table S2 online). Following GaM treatment, we identified four genes within the oxidative stress pathway and three genes within the p53 pathway (Figure 4a) that were differentially expressed. In particular, expression of heme oxygenase 1 (Exner *et al.*, 2004), a fundamental gene involved in the activation of the oxidative stress pathway, was increased in GaM-treated Hut78 cells versus controls by both real-time reverse-transcriptase–PCR and western blot (Supplementary Figure S6 online). CDKN1A (p21; Harper *et al.*, 1993) and GADD45A (Salvador *et al.*, 2013), two p53 pathway genes found to be

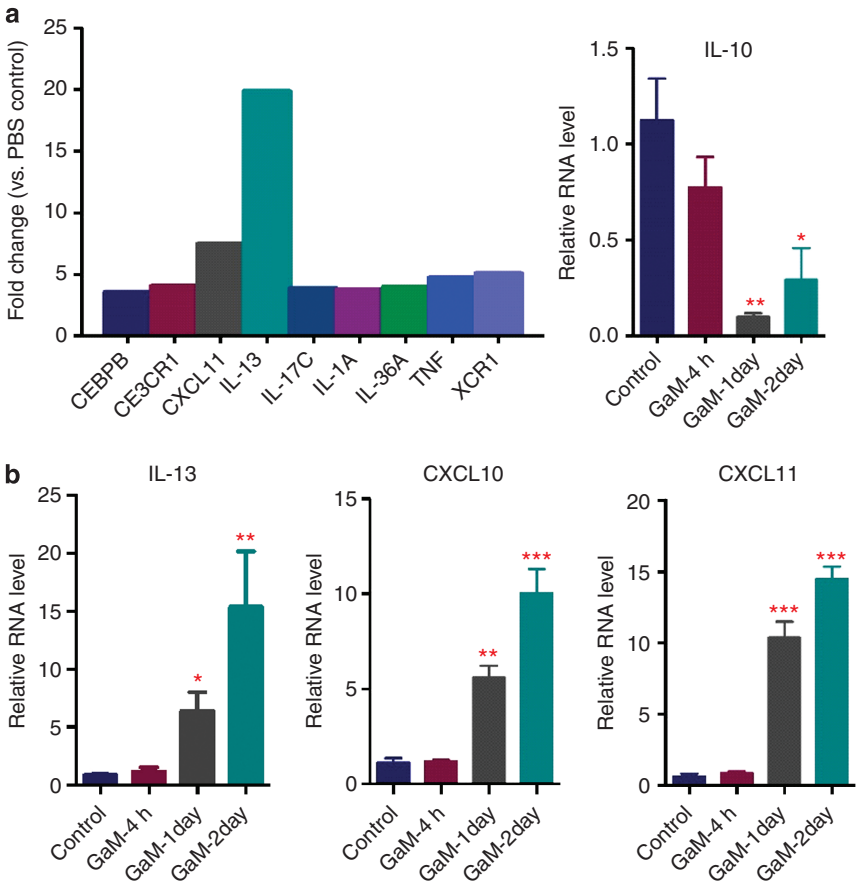

Figure 3. Gallium maltolate (GaM) alters expression levels of inflammatory cytokines in Hut78 cells. (**a**) Upregulated genes in GaM vs. PBS-treated Hut78 cells by inflammatory cytokines and receptor PCR array (fold change >2.5). (**b**) Real-time PCR analysis of the expression levels of IL-10, IL-13, CXCL10, and 11 in GAM/PBS-treated Hut78 cells. y-Axis shows relative quantification after correction to glyceraldehyde-3-phosphate dehydrogenase expression. *$P<0.05$, **$P<0.001$, and ***$P<0.0001$ compared with the control group.

7–8-fold upregulated, mediate growth arrest following cellular stress. BTG2, a member of a family that appears to have anti-proliferative properties (Rouault *et al.*, 1996), was also found to be ~3-fold upregulated (Figure 4a). In addition, because GADD45A is believed to activate the p38/JNK (c-Jun N-terminal kinase) pathway and lead to apoptosis when responding to environmental stress, we measured phosphorylated p38 in CTCL cells incubated with GaM. Western blot showed an increase in phospho-p38 in Hut78 cells after 24 hours in culture with 100 μM GaM (Figure 4b). Thus, GaM clearly alters key signaling pathways that may facilitate apoptosis of CTCL cells.

DISCUSSION

GaM has gained attention for its potent anti-inflammatory and anti-tumor activities. It shows high bioavailability in multiple formulations including oral, topical, and other routes of administration, making it an attractive therapeutic agent. Compared with GaN, GaM shows significantly greater cytotoxicity in tumor cells *in vitro,* and most importantly it is capable of inducing apoptosis in cells that are resistant to GaN (Chitambar *et al.*, 2007). Herein, we report that GaM effectively induced CTCL cell apoptosis and inhibited CTCL tumor formation in an animal model using *bona fide* human CTCL cells.

Although gallium shares similarities with iron with respect to ionic radius, binding to transferrin and certain other iron-binding proteins, and incorporation into cells by the TfR-mediated pathway, it does not appear to have a functional role in mammalian cells. Instead, gallium interferes with the function of iron-containing cellular proteins, leading to a disruption of iron homeostasis in cells. Because malignant cells exhibit a greater metabolic requirement for iron, gallium compounds are more cytotoxic to proliferating malignant cells relative to normal cells. We have assessed the toxicity of GaM toward HaCaT cells (Supplementary Figure S2 online), a non-malignant keratinocyte cell line, and found that GaM showed far less toxicity toward HaCaT cells. When administered in mouse skin, GaM did not induce erosion or necrosis in normal skin, although we did observe mild skin edema and redness (data not shown). These observations suggest that GaM-based anti-tumor therapy may have limited toxicity to surrounding normal cells.

A clinically useful CTCL treatment must be able to reduce the growth of established tumors. We used a human CTCL xenograft model in NSG mice to determine the efficacy of

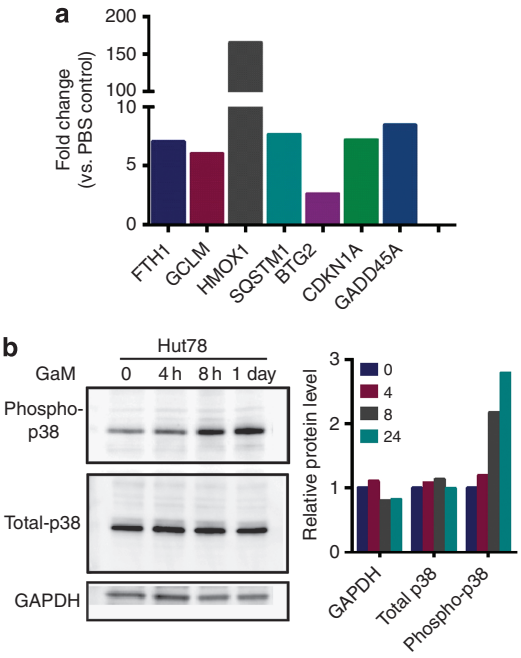

Figure 4. GaM treatment activates oxidative stress and p53 pathways in Hut78 cells. (**a**) Upregulated genes in GaM vs. PBS-treated Hut78 cells by Pathway Finder PCR array (fold change >2.5). (**b**) Activation of the p38/MAPK pathway was detected by western blot in GaM-treated CTCL cell. Image acquisition and analysis was carried out through Image Lab software.

GaM treatment at different time periods after tumor inoculation. Of note, the results showed that up to 60% of mice were protected from tumor formation by GaM administration in the first week treatment group. Moreover, reductions in tumor size were observed in the 2nd and even in the 3rd week treatment groups, validating the effectiveness of GaM in established CTCL tumors.

Inflammatory cytokines are important molecules that mediate both tumor growth and host anti-tumor immunity. Tumor cells usually enhance the production of specific types of cytokines that help the tumor cells survive host immune responses. In this case, we detected reproducible changes in the inflammatory cytokine profile of GaM-treated CTCL cells. We found that GaM treatment increased the IFN-γ-inducible chemokines, CXCL10 and CXCL11, which attract $CXCR3^+$ Th1 lymphocytes and inhibit angiogenesis (Tannenbaum *et al.*, 1998; Hensbergen *et al.*, 2005). Of note, CXCL10 (IP-10) has been described as a potent angiostatic factor that regulates tumor angiogenesis and inhibits tumorigenesis and tumor metastasis (Arenberg *et al.*, 1996). Expression of IL-13, a cytokine that promotes host immune surveillance and tumor immunity (Serve *et al.*, 1996, Volpert *et al.*, 1998), was also greatly induced following GaM treatment. Finally, IL-10, a Th2 cytokine that promotes angiogenesis, was found to be downregulated following GaM treatment. IL-10 has been shown to be upregulated in the setting of clinical progression of mycosis fungoides (Asadullah *et al.*, 1996). Thus, the cytokine profile shift that we observed with GaM treatment would help create an unfavorable environment for tumor growth by decreasing angiogenesis and increasing migration of anti-tumor immune cells into the tumor.

In exploring downstream signaling pathways that may be involved in apoptosis of CTCL cells induced by GaM, we identified activation of representative genes in both oxidative stress and p53 pathways in Hut78 cells with GaM treatment. Oxidative stress driven by inflammation results in an excess of free radical species, leading to cellular injury and death. Specifically, the marked upregulation of heme oxygenase 1, one of the most important genes in the oxidative stress pathway, was confirmed in GaM-treated Hut78 CTCL cells. Upregulation of heme oxygenase 1 serves as an adaptive mechanism to protect cells from oxidative damage, suggesting that GaM can induce cellular defensive mechanisms as a byproduct of cytotoxicity. We also identified involvement of the p53 pathway following GaM treatment. As a representative gene for p53 pathway, GADD45A was increased at transcriptional levels following stressful growth arrest conditions and treatment with DNA-damaging agents (Salvador *et al.*, 2013). The protein encoded by this gene responds to environmental stressors by activating the p38/JNK pathway (Zhu *et al.*, 2009), which we confirmed by detection of phosphorylated p38 in GaM-treated CTCL cells.

In summary, our results clearly demonstrate that GaM treatment *in vivo* blocks growth of (established) human CTCL tumors in xenograft models. Mechanistically, multiple immunologic and metabolic changes following administration of GaM produce an environment that favors anti-tumor responses and increases cellular metabolic stress. Agents that work via multiple mechanisms may decrease the potential for cancer cells to develop resistance. Further investigation of gallium-containing compounds, including GaM, is indicated in order to improve the therapeutic arsenal for advanced CTCL.

MATERIALS AND METHODS

Animals and cell lines

Female NSG (stock number 005557) mice (8–10-week old) were purchased from Jackson Laboratory (Bar Harbor, ME). Mice were housed at the Medical College of Wisconsin in the barrier animal room with sterilization of food, bedding, and supplies. All animal experiments were conducted in accordance with the guidelines and approval of the Institutional Animal Care and Usage Committee (IACUC) at the Medical College of Wisconsin. Human CTCL cell lines, Hut78 and HH, were purchased from ATCC (Manassas, VA; Cat number: TIB-161 and CRL-2105). Hut78 cells were cultured in Iscove's Modified Dulbecco's medium. HH cells were cultured in RPMI-1640 medium.

Flow cytometric analysis and apoptosis detection

TfR antibodies (anti-human CD71 and anti-mouse CD71), anti-CD45, anti-mouse F4/80, and anti-mouse Gr-1 were purchased from BioLegend (San Diego, CA). The Apoptosis detection PE kit was purchased from eBioscience (San Diego, CA). In order to detect surface markers, cells were washed once in PBS, once in FACS buffer, and resuspended in FACS buffer at $5 \times 10^5\,ml^{-1}$. Cells were then incubated with antibodies at 4 °C for 30 min and washed with FACS buffer. Cell preparation was analyzed on a BD FACSCalibur flow

cytometer (San Jose, CA). For apoptosis detection, GAM-treated/untreated cells were washed once in PBS, once in 1x Binding Buffer, and resuspended in 1x Binding Buffer at $5 \times 10^6\,ml^{-1}$. PE-conjugated Annexin V (5 µl) was added to 100 µl of the cell suspension and incubated for 10–15 minutes at room temperature. Cells were washed in 1x Binding Buffer and resuspended in 200 µl of 1x Binding Buffer. A volume of 5 µl of 7-AAD Viability staining solution was added, and the cells were immediately analyzed by flow cytometry.

Mitochondrial oxygen consumption

The effects of GaM on mitochondrial function was assessed by measuring the oxygen consumption rate in intact HuT78 cells using a Seahorse XF24 Extracellular Flux Analyzer according to the manufacturer's recommendations (Dranka *et al.*, 2011). Cells were incubated in tissue culture with increasing concentrations of GaM for 8 hours and then collected, washed in Dulbecco's PBS, and resuspended in unbuffered RPMI-1640 assay media containing 2 mM L-glutamine, 5 mM sodium pyruvate, pH 7.4, without sodium bicarbonate (Life Technologies; Grand Island, NY). Cells (750,000 cells per well) were plated in Seahorse Bioscience V7 tissue culture plates. One hundred microliters of cell suspension in non-buffered assay media was added per well to be measured. Prior to seeding, the assay plates were coated with Cell-Tak (BD Biosciences; San Jose, CA). Cells were centrifuged to the bottom of the plate at $250 \times g$ for 5 minutes prior to the addition of an additional 400 µl of assay media.

Establishment of tumor mouse models and GaM treatment

Mice were sedated with IP injection of ketamine/xylazine solution. PBS–washed CTCL cells (Hut78 or HH) (1×10^6 per mouse) were injected into the SC space in the center of the shaved skin using a 28 g needle. Mice were monitored during recovery from anesthesia and moved back to normal housing. Tumors were visually examined twice a week until the end point in the 4th week after implantation. For *in vivo* GaM treatment, daily injections were performed for 5 days. Depending on the initiation of GaM administration, three treatment regimens were used: 1st week, 2nd week, and 3rd week treatment, which started on day 2, 8, and 15, respectively, after tumor cell implantation on day 1, were performed (Figure 2a). All GaM treatments involved careful injection of GaM (five consecutive daily injection, 400 µg per injection) into the SC tissue around the site of tumor implantation (peritumoral injection) while avoiding the tumor mass itself. For the control group, equal volumes of PBS (200 µl) were injected in similar manner.

Western blot

CTCL cells treated with and without GaM were collected, lysed, and centrifuged to remove cellular debris. The protein content of supernatants was measured by the bicinchoninic acid protein assay (Pierce, Rockford, IL). Samples were resolved by NuPAGE Bis-Tris precast gel and transferred into a nitrocellulose membrane using a Transblot system (Life Technologies). Membranes were incubated with specific primary antibody to p38, phosphorylated p38, HO-1, and glyceraldehyde-3-phosphate dehydrogenase. Washed membranes were incubated in appropriate secondary antibody conjugated to horseradish peroxidase, immersed in Pierce ECL chemiluminescence detection solution (Pierce), and recorded by imaging with a Molecular Imager Gel Doc XR+ system with Image Lab Software (Bio-Rad, Hercules, CA).

CONFLICT OF INTEREST

The authors state no conflict of interest.

ACKNOWLEDGMENTS

We thank Wasakorn Kittipongdaja and Brian Schulte for their critical reading and helpful language editing.

SUPPLEMENTARY MATERIAL

Supplementary material is linked to the online version of the paper at http://www.nature.com/jid

REFERENCES

Arenberg DA, Kunkel SL, Polverini PJ *et al.* (1996) Interferon-gamma-inducible protein 10 (IP-10) is an angiostatic factor that inhibits human non-small cell lung cancer (NSCLC) tumorigenesis and spontaneous metastases. *J Exp Med* 184:981–92

Asadullah K, Docke WD, Haeussler A *et al.* (1996) Progression of mycosis fungoides is associated with increasing cutaneous expression of interleukin-10 mRNA. *J Invest Dermatol* 107:833–7

Chitambar CR (2012) Gallium-containing anticancer compounds. *Future Med Chem* 4:1257–72

Chitambar CR (2010) Medical applications and toxicities of gallium compounds. *Int J Environ Res Public Health* 7:2337–61

Chitambar CR, Antholine WE (2013) Iron-targeting antitumor activity of gallium compounds and novel insights into triapine((R))-metal complexes. *Antioxid Redox Signal* 18:956–72

Chitambar CR, Purpi DP, Woodliff J *et al.* (2007) Development of gallium compounds for treatment of lymphoma: Gallium maltolate, a novel hydroxypyrone gallium compound, induces apoptosis and circumvents lymphoma cell resistance to gallium nitrate. *J Pharmacol Exp Ther* 322:1228–36

Chitambar CR, Seigneuret MC, Matthaeus WG *et al.* (1989) Modulation of lymphocyte proliferation and immunoglobulin production by transferrin-gallium. *Cancer Res* 49:1125–9

Chitambar CR, Zivkovic Z (1987) Uptake of gallium-67 by human leukemic cells: Demonstration of transferrin receptor-dependent and transferrin-independent mechanisms. *Cancer Res* 47:3929–34

Dranka BP, Benavides GA, Diers AR *et al.* (2011) Assessing bioenergetic function in response to oxidative stress by metabolic profiling. *Free Radic Biol Med* 51:1621–35

Exner M, Minar E, Wagner O *et al.* (2004) The role of heme oxygenase-1 promoter polymorphisms in human disease. *Free Radic Biol Med* 37:1097–104

Harper JW, Adami GR, Wei N *et al.* (1993) The p21 cdk-interacting protein Cip1 is a potent inhibitor of G1 cyclin-dependent kinases. *Cell* 75:805–16

Harris WR, Pecoraro VL (1983) Thermodynamic binding constants for gallium transferrin. *Biochemistry* 22:292–9

Hensbergen PJ, Wijnands PG, Schreurs MW *et al.* (2005) The CXCR3 targeting chemokine CXCL11 has potent antitumor activity *in vivo* involving attraction of CD8+ T lymphocytes but not inhibition of angiogenesis. *J Immunother* 28:343–51

Huang Z, Higgins B, Foss F (2005) Activity of gallium nitrate in refractory peripheral T-cell lymphoma. *Clin Lymphoma* 6:43–5

Hwang ST, Janik JE, Jaffe ES *et al.* (2008) Mycosis fungoides and sezary syndrome. *Lancet* 371:945–57

Kvaloy S, Langholm R, Kaalhus O *et al.* (1984) Transferrin receptor and B-lymphoblast antigen–their relationship to DNA synthesis, histology and survival in B-cell lymphomas. *Int J Cancer* 33:173–7

Larson SM, Rasey JS, Allen DR *et al.* (1980) Common pathway for tumor cell uptake of gallium-67 and iron-59 via a transferrin receptor. *J Natl Cancer Inst* 64:41–53

Mantovani A, Allavena P, Sica A *et al.* (2008) Cancer-related inflammation. *Nature* 454:436–44

Richardson DR, Kalinowski DS, Lau S *et al.* (2009) Cancer cell iron metabolism and the development of potent iron chelators as anti-tumour agents. *Biochim Biophys Acta* 1790:702–17

Rouault JP, Falette N, Guehenneux F *et al.* (1996) Identification of BTG2, an antiproliferative p53-dependent component of the DNA damage cellular response pathway. *Nat Genet* 14:482–6

Salvador JM, Brown-Clay JD, Fornace AJ Jr (2013) Gadd45 in stress signaling, cell cycle control, and apoptosis. *Adv Exp Med Biol* 793:1–19

Serve H, Oelmann E, Herweg A *et al.* (1996) Inhibition of proliferation and clonal growth of human breast cancer cells by interleukin 13. *Cancer Res* 56:3583–8

Straus DJ (2003) Gallium nitrate in the treatment of lymphoma. *Semin Oncol* 30:25–33

Sugaya M, Miyagaki T, Ohmatsu H *et al.* (2012) Association of the numbers of CD163(+) cells in lesional skin and serum levels of soluble CD163 with disease progression of cutaneous T cell lymphoma. *J Dermatol Sci* 68:45–51

Tannenbaum CS, Tubbs R, Armstrong D *et al.* (1998) The CXC chemokines IP-10 and mig are necessary for IL-12-mediated regression of the mouse RENCA tumor. *J Immunol* 161:927–32

Volpert OV, Fong T, Koch AE *et al.* (1998) Inhibition of angiogenesis by interleukin 4. *J Exp Med* 188:1039–46

Wu X, Schulte BC, Zhou Y *et al.* (2014) Depletion of M2-like tumor-associated macrophages delays cutaneous T-cell lymphoma development *in vivo*. *J Invest Dermatol* 134:2814–22

Wu X, Sells RE, Hwang ST (2011) Upregulation of inflammatory cytokines and oncogenic signal pathways preceding tumor formation in a murine model of T-cell lymphoma in skin. *J Invest Dermatol* 131:1727–34

Zhu N, Shao Y, Xu L *et al.* (2009) Gadd45-alpha and Gadd45-gamma utilize p38 and JNK signaling pathways to induce cell cycle G2/M arrest in hep-G2 hepatoma cells. *Mol Biol Rep* 36:2075–85